

Structural and magnetic properties of molecular beam epitaxy $(\text{MnSb}_2\text{Te}_4)_x(\text{Sb}_2\text{Te}_3)_{1-x}$ topological materials with exceedingly high Curie temperature

**Candice R. Forrester,^{1,2,3} Christophe Testelin,⁴ Kaushini Wickramasinghe,¹ Ido Levy,⁵
Dominique Demaille,⁴ David Hrabovsky,⁶ Xiaxin Ding,⁷ Lia Krusin-Elbaum,^{7,8}
Gustavo E. Lopez,^{2,3} Maria C. Tamargo^{1,2}**

¹Department of Chemistry, The City College of New York, NY, NY 10031

²PhD Program in Chemistry, CUNY Graduate Center, NY, NY 10016

³Department of Chemistry, Lehman College, Bronx, NY 10468

⁴Sorbonne Université, CNRS, Institut des NanoScience de Paris, F-75005 Paris, France

⁵Department of Physics, New York University, NY, NY 10003

⁶Sorbonne Université, MPBT Platform, 4 Place Jussieu, 75252 Paris, France

⁷Department of Physics, The City College of New York, NY, NY 10031

⁸ PhD Program in Physics, CUNY Graduate Center, NY, NY 10016

SLOW GROWTH RATE

FAST GROWTH RATE

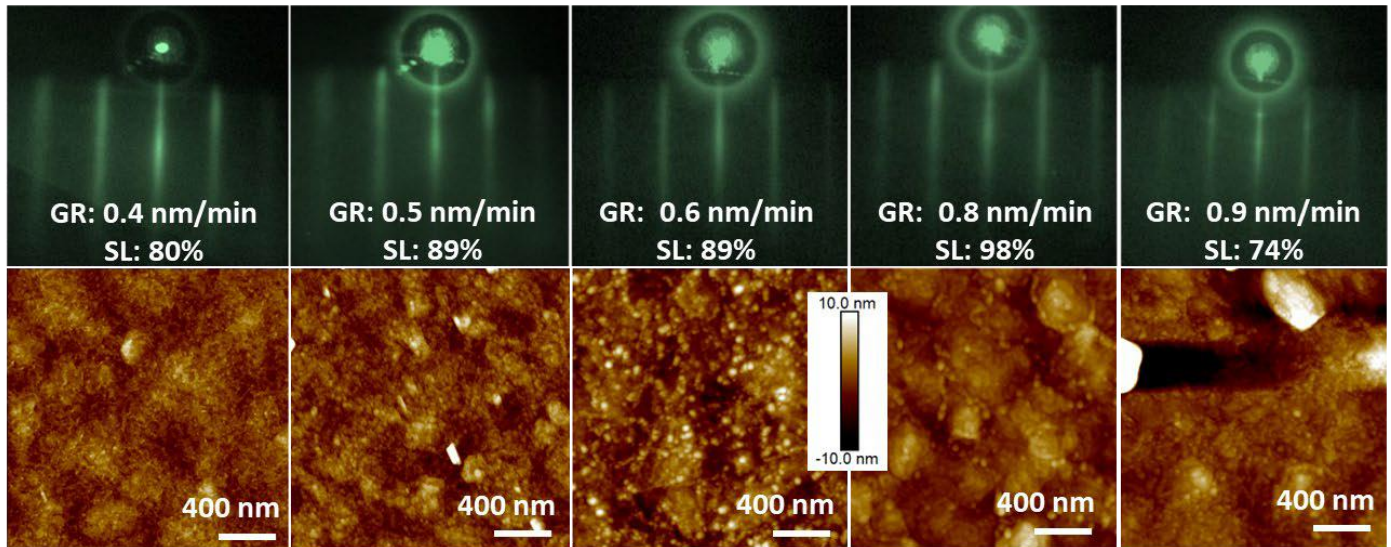


Figure S1: RHEED (top) and AFM images (bottom) of $(\text{Sb}_2\text{Te}_3)_{1-x}(\text{MnSb}_2\text{Te}_4)_x$ samples grown with increasing growth rates. Samples grown with a slower growth rate are on the left and samples grown with faster growth rates are on the right. No significant changes in the RHEED and AFM were observed as the growth rate changed.

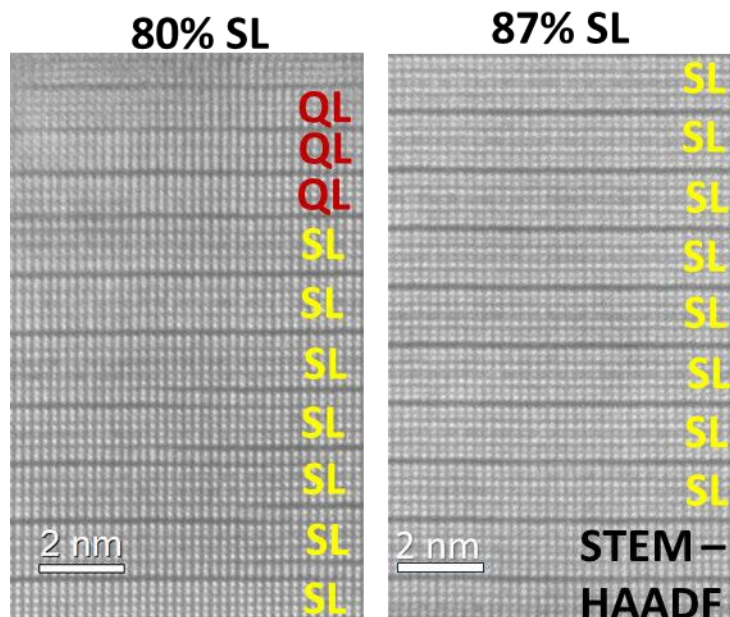


Figure S2. Cross-sectional STEM images of two samples $(\text{Sb}_2\text{Te}_3)_{1-x}(\text{MnSb}_2\text{Te}_4)_x$ with $x > 0.7$ grown with slow growth rates. Good crystalline quality is observed in the samples.

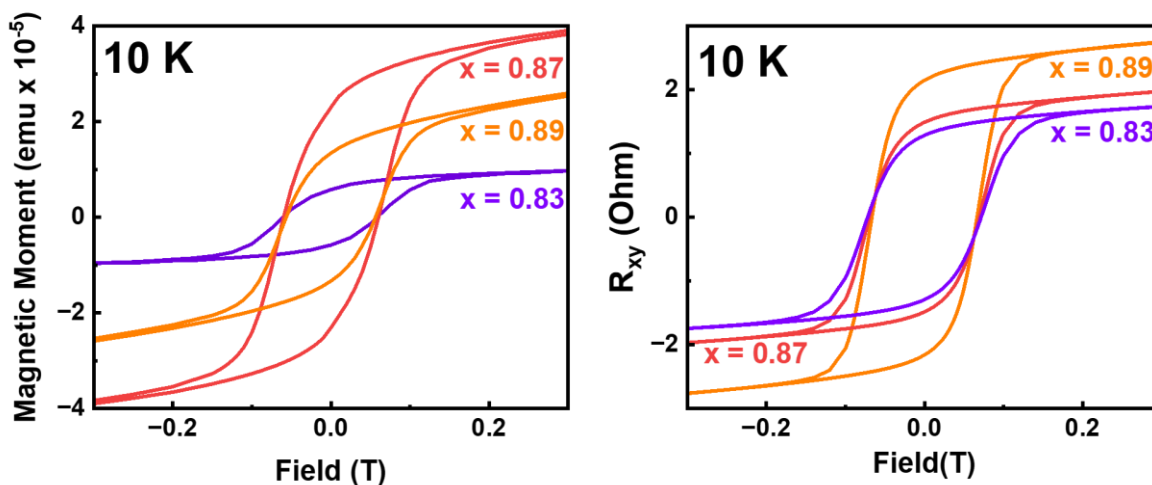


Figure S3: Field dependent magnetization (left) and Hall resistance (right) measurements taken at 10K for samples of $(\text{Sb}_2\text{Te}_3)_{1-x}(\text{MnSb}_2\text{Te}_4)_x$ in which $x \geq 0.7$. Hysteretic loops which indicate ferromagnetic behavior are consistently seen in both measurements. The curves labelled $x = 0.83$ on each plot are for the same sample, which exhibits high T_C in the manuscript (shown in Figures 2e and 2f), and the curves labelled $x = 0.89$ are for the sample shown in Figure 3 of the manuscript.

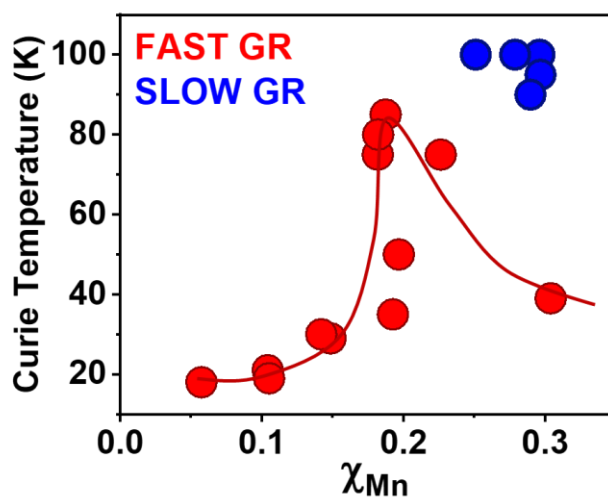


Figure S4: The Curie temperature plotted vs the Mn fraction (χ_{Mn}) as measured by EDS for a subset of the samples of $(\text{Sb}_{2-y}\text{Mn}_y\text{Te}_3)_{1-x}(\text{Mn}_{1+y}\text{Sb}_{2-y}\text{Te}_4)_x$ shown in Figure 4c of the main text. In Fig. 4c the data are plotted vs composition (x). The line is drawn to aid the eye. A similar trend is seen here as in Figure 4c. This plot highlights the importance of Mn fraction to enhance the T_C , especially as it compares the slow growth rate samples with the fast growth rate samples. By contrast, the plot of Figure 4c illustrates the importance of the composition x . Both factors are influential in determining the exceedingly high T_C values observed in our study.

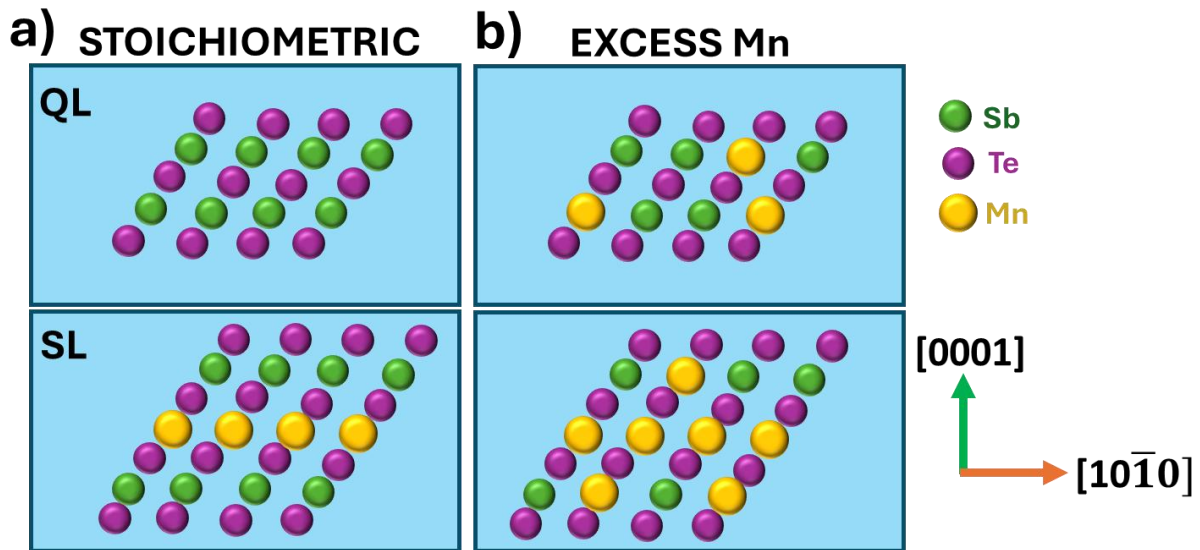


Figure S5: Atomic arrangement of the elements in the $(\text{MnSb}_2\text{Te}_4)_x(\text{Sb}_2\text{Te}_3)_{1-x}$ samples discussed in the text. The vertical direction in the panels corresponds to the growth direction $[0001]$, perpendicular to the van der Waals gaps (vdW), and the $[10\bar{1}0]$ direction is parallel to the vdW gaps. a) Atomic arrangements of a quintuple layer (QL) of Sb_2Te_3 (top panel) and a septuple layer (SL) of MnSb_2Te_4 (bottom panel), *without excess Mn* (stoichiometric). The Mn atoms appear only in the middle row of the SL. b) Atomic arrangement of a $\text{Sb}_{2-y}\text{Mn}_y\text{Te}_3$ QL structure *with excess Mn* shown as substitutional Mn atoms in Sb sites (top panel) and a $\text{Mn}_{1+y}\text{Sb}_{2-y}\text{Te}_4$ SL structure, with excess Mn shown as substitutional Mn atoms in Sb sites (bottom panel). Excess Mn is observed in both the SLs and the QLs.